JAERI 1138

JAERI 1138

The Neutron Time-of-Flight Spectrometer at JAERI Linac

August 1967

日本原子力研究所

Japan Atomic Energy Research Institute

日本原子力研究所は，研究成果，調査結果の報告のため，つぎの3種の研究報告書を，それぞれの通しナンバーを付して，不定期に公刊しております．

1. 研究報告	まとまった研究の成果あるいはその一部における重要な結果の報告	JAERI 1001-3999
2. 調査報告	総説，展望，紹介などを含め，研究の成果 調査の結果をまとめたもの	JAERI 4001-5999
3. 資　　料	研究成果の普及，開発状況の紹介，施設共同利用の手引など	JAERI 6001-6999

このうち既刊分については「JAERI レポード一覧」にタイトル・要旨をまとめて掲載し，また新刊レポートは「原研びぶりお」でその都度紹介しています．これらの研究報告書に関する頒布，版権，複写のお問合せは，日本原子力研究所技術情報部（茨城県那珂郡東海村）あてお申し越しください．

Japan Atomic Energy Research Institute publishes the nonperiodical reports with the following classification numbers:

1. **JAERI** 1001-3999 Research reports,
2. **JAERI** 4001-5999 Survey reports and reviews,
3. **JAERI** 6001-6999 Information and Guiding Booklets.

Any inquiries concerning distribution copyright and reprint of the above reports should be derected to the Division of Technical Information, Japan Atomic Energy Research Institute, Tokai-mura, Naka-gun, Ibaraki-ken, Japan.

編集兼発行　日本原子力研究所

The Neutron Time-of-Flight Spectrometer at JAERI Linac

Abstract

The physical arrangements and characteristics of the neutron time-of-flight spectrometer installation at the JAERI 20-Mev Electron Linac are described. Pulsed neutron beam is produced at a photoneutron target by the linac-electron pulses, whose width is chosen to be of any value from 4 μsec to 40 nsec, and the neutrons are detected, through evacuated flight tubes, by a neutron detector composed of ^{6}Li-glass scintillators at 50 meters from the source target. The flight time of neutrons between the target and the detector is measured by a 4096-channel time analyzer. Characteristics of the neutron detector, spectrum of the neutron beam, background, resolution, monitoring of the neutron beam, data processing, and typical data of the neutron transmission are also reported.

April 1967

A. Asami, T. Fuketa, Y. Kawarasaki, Y. Nakajima,
M. Okubo, T. Sakuta, K. Takahashi, and H. Takekoshi
Linac Laboratory, Division of Research
Tokai Research Establishment
Japan Atomic Energy Research Institute

原研リニアックにおける
中性子タイム・オブ・フライト・スペクトロメータ

要　旨

パルス状中性子ビームは 4 μsec から 40 nsec の間の任意の値の幅に選ばれたリニアック電子パルスによって光中性子ターゲットにおいて発生し，真空飛行管を通してターゲットから 50 メートルの距離にある ^{6}Li ガラス・シンチレータからなる中性子検出器によって検出される．ターゲットと検出器との間の中性子飛行時間は，4096-チャネル時間分析器によって測定される．中性子検出器の特性，中性子ビームのスペクトル，バックグラウンド，分解能，ビームのモニタリング，データ処理，中性子透過率のデータ例などについて報告する．

1967 年 4 月

日本原子力研究所　東海研究所
研究部原子核物理第 2 研究室
浅見明，更田豊治郎，河原崎雄紀，中島豊，
大久保牧夫，作田孝，高橋興起，竹腰秀邦

Contents

目　次

1. Introduction

Researches on interactions between slow neutrons and nuclei have been made strenuously at laboratories in various countries for the purpose of obtaining fundamental knowledge of the interaction and with a view to meet the demand of nuclear data necessary for designing nuclear reactors. In these research works, accumulation of a mass of various basic data, such as of cross section and resonance parameters, has been achieved. These data have been used for the reactor designing either directly or in forms of reactor constants which are evaluated from the original nuclear data, and systematic investigations on these data have revealed the mechanism of compound-nucleus formation by *s*-wave neutrons.

Systematics of the average level spacings and widths, and strength functions upon the nucleon numbers of nuclei is treated by many theoretical works on the basis of nuclear optical and shell models; and, the WIGNER distribution[1] and the PORTER-THOMAS distribution[2] are generally accepted to represent distribution of the nearest-neighbour level-spacings and that of the reduced neutron widths, respectively. Recent progress in increasing intensity of pulsed-neutron sources especially with high power electron linacs and in measurement techniques has stimulated the measurements of various types (total and partial) of neutron cross sections. Consequently, while the accumulation and the accuracy of the data have been increased rapidly, a number of investigations have been aimed at more detailed relations[3] among neutron-resonance parameters and at relatively new problems: spin dependence of the strength function[4], distribution of the partial radiation widths[5], *p*-wave resonances in slow-neutron energy range[6], direct process at neutron capture[7], existence of the doorway states to the neutron resonances[8], and so on.

Most of these measurements have been made by the method of neutron time of flight (TOF). Reactors with rotating choppers were mostly used as the pulsed neutron sources in the early days. On the other hand, owing to the recent progress in techniques of microwave and of manufacturing high power klystrons, electron linacs of high power and high reliability have been constructed in various countries. Besides its high intensity of neutron bursts, the linac has an excellent characteristics as a pulsed neutron source, that is, the width and the repetition rate of the neutron bursts are easily controlled and the very short width is obtained by electric deflection or bunching of the electron beam at the electron gun. In recent years, therefore, the pulsed neutron sources of the slow neutron TOF spectrometers tend to be monopolized by the linacs. The use of the Columbia University Nevis Synchrocyclotron for neutron TOF studies[9] is the remarkable exception of the above statement.

The neutron physics experiments with the linac have been carried out at A.E.R.E., Harwell for a long time, during that time the linac was reinforced and many experimental results have been obtained[10]. At present, linacs of 30- to 60-MeV nominal energy are in operation at C.E.N. at Saclay, General Atomic, R.P.I., C.B.M.N. at Geel, Kurchatov Institute, and others almost exclusively for neutron physics. At the ORNL, where a fast chopper has been operated for many years, a powerful linac of 150 MeV and the peak current of fifteen amperes is going to be constructed[11].

The construction of the 20-MeV JAERI Linac was completed at the end of 1960 under the initial programme of using it rather generally for physics research, production of activities, and electron irradiation. The preliminary experiment of the neutron TOF method was started in 1961 with a 10-m flight path and a 256-channel time analyzer, and a flight tube of 50-m path length was installed in 1963. Since the installation of a 4096-channel time analyzer in 1965, processing and analysis of the experimental data by using an IBM-7044 computer have been made progress; and, total cross-

section measurements on cobalt, cadmium, and antimony have been performed by now. The results of these measurements are to be published elsewhere.

2. Linac and the beam pulse forming

The JAERI Electron Linac[12] is of *s*-band travelling wave type and was manufactured by the High Voltage Engineering Corporation, U.S.A. Its electron output energy is 20 MeV nominal and 26 MeV at maximum. The cathode of the electron gun is of directly-heated type and made of tantalum filament, and electron current is taken out by applying voltage pulses of −60 KV and 5-μsec width. The electron beam is pulsed by a pair of deflecting plates which is located between the electron gun and the accelerator tube. The electron beam from the gun does not enter to the accelerator tube when a voltage of about 10 kV is applied to the deflector. The beam enters into the accelerator tube only when the deflection is released by a rectangular voltage pulse, whose width can be chosen to any value between 4 μsec and 40 nsec. When the pulse width shorter than 40 nsec is required, the electron beam is swept by the rising portion of voltage pulse applied to the deflector.

The accelerated electron beam is brought to a target room through the beam duct, and is emitted into air through a window of 0.1-mm thick aluminium foil. A ferrite ring is mounted at the outside of the window, and a signal pulse is obtained from several turns of coil around the ring when the beam pulse passes it. This signal is used as the zero-time signal to trigger the time analyzer. The ferrite core is subjected to exchange in a few months because of deterioration of its magnetic permeability by radiation damage*. When the accelerator tubes are energized by 6 MW microwave power, the peak currents of 150 mA and 380 mA are obtained with the pulse widths of 4 μsec, and 0.05 μsec, respectively. The energy spectra of the pulsed electron beams are exemplified in Fig. 1.

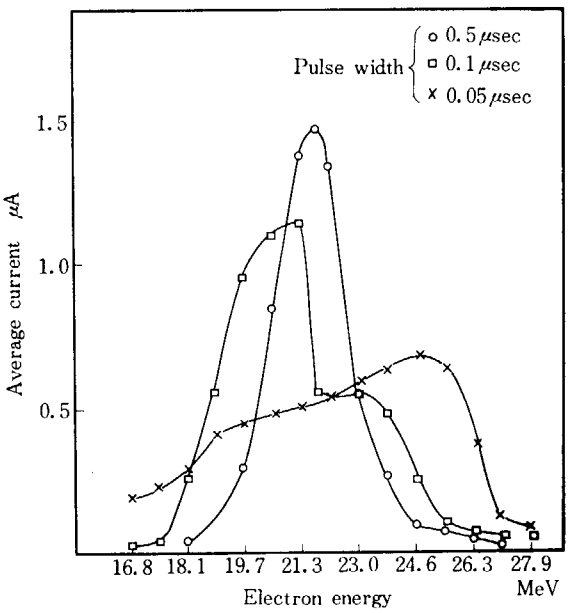

Fig. 1 Example of the energy spectra of the pulsed electron beams from the linac. Widths of the pulsed beams are shown in the figure. For shorter pulse width, there seems to be tendency that the energy and its spread result in higher and broader, respectively.

*This deterioration of permeability is found to be recovered to a certain extent as time goes on under the condition of no irradiation.

3. Instrumentation of TOF equipments

The scheme of the neutron time-of-flight spectrometer is shown in Fig. 2. Photoneutrons produced at the target are moderated by hydrogenous material. At present, two flight paths are utilized: the one has a path length of 50 meters at angle of 100° to the direction of the electron beam and the other of 10 m at 115°. The longer flight path goes out of the main building and reaches a shack of detector at the end of the path. The target room is shielded by heavy-concrete blocks with thicknesses of 3 to 4 m at the wall and 0.8 m at the ceiling. Time analyzer and other measuring electronics are

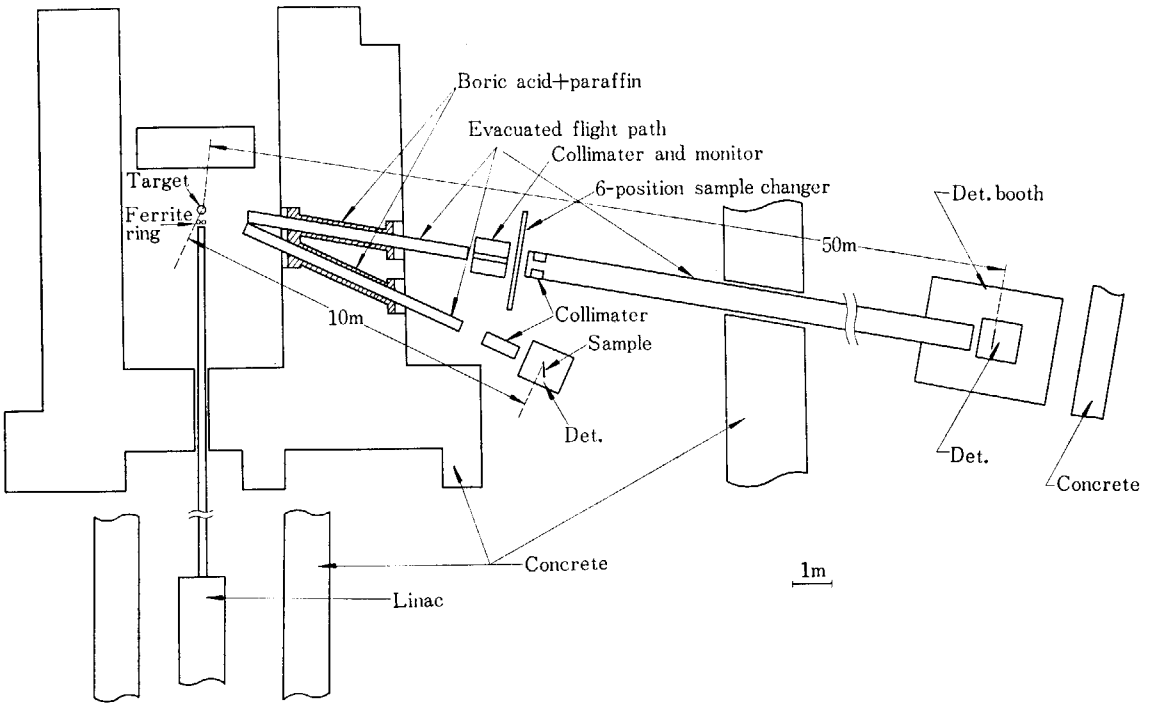

Fig. 2 The scheme of the neutron time-of-flight spectrometer.
(a) Schematic diagram of the spectrometer

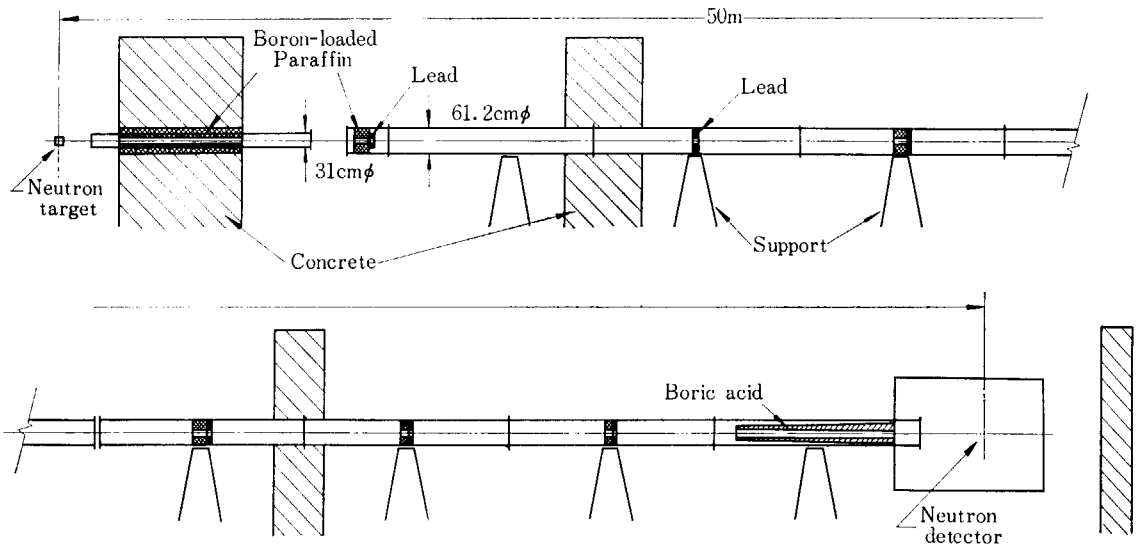

(d) Illustration of the flight tubes and collimators of the 50-m flight path

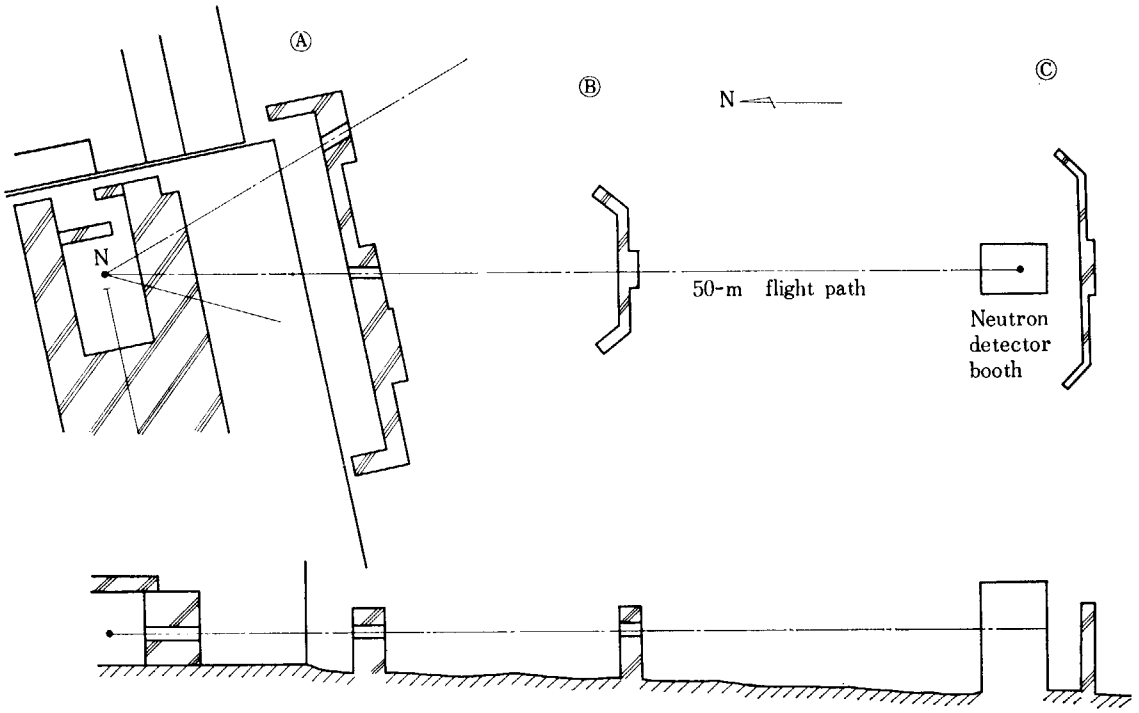

(c) Simplified ground-plan of the shielding arrangement

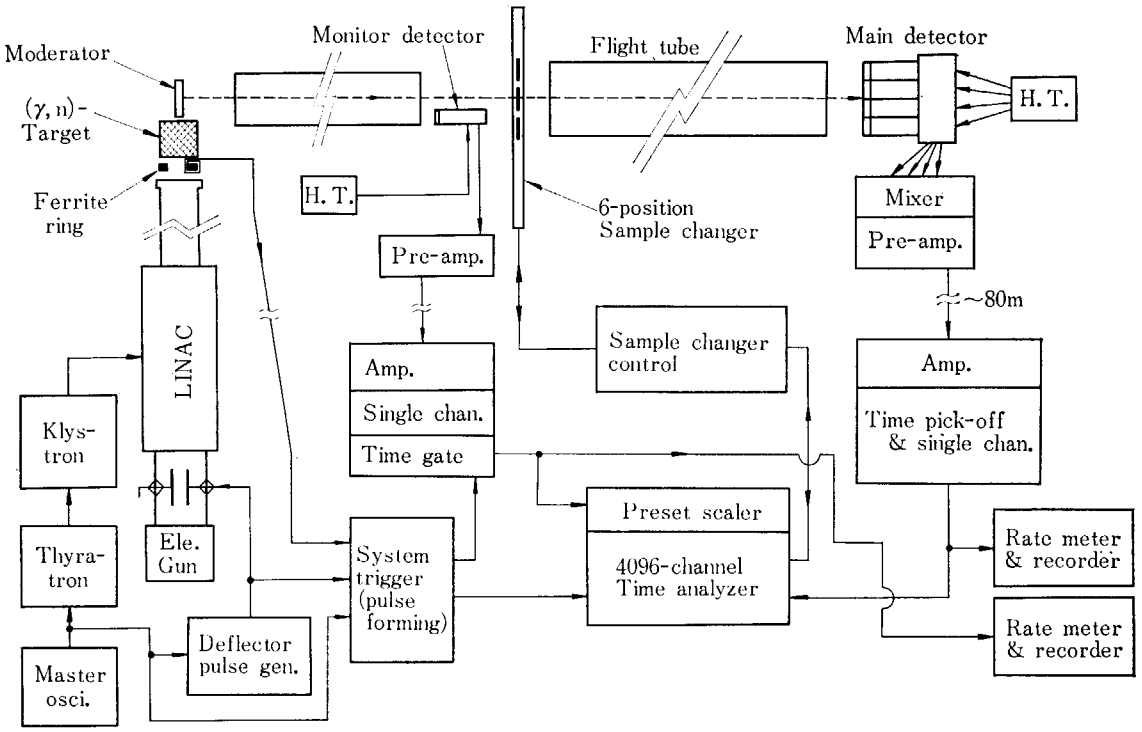

(d) Block diagram of the electronic system

located at the control room of the Linac. Detailed descriptions of the main instrumentation are made in the following.

3. 1 Target

A sketch of the assembly of the photo-neutron source target is shown in Fig. 3. Lead is used to produce bremsstrahlung and photoneutrons, and the assembly is canned in a stainless steel vessel

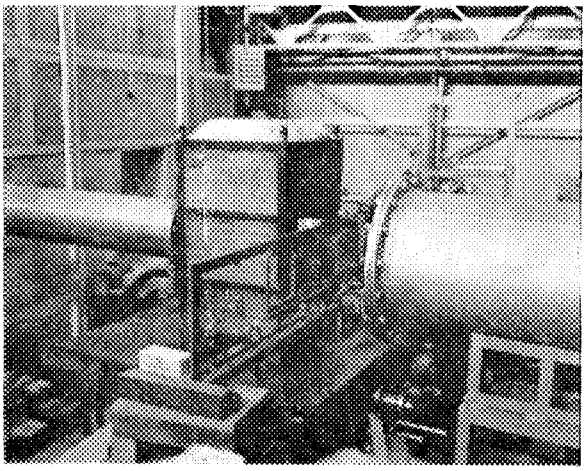

Fig. 2 (e) The collimator assembly and the six-position sample changer

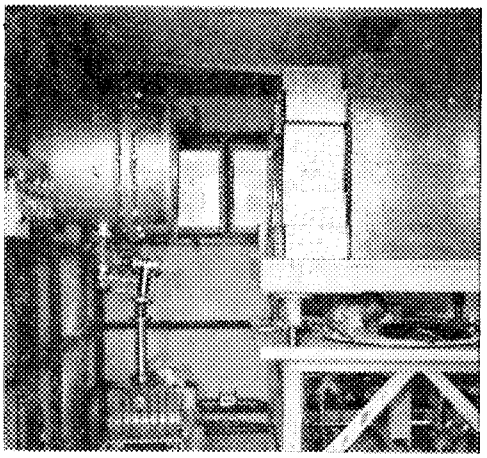

Fig. 2 (f) The end of the 50-m flight tube and the detector shielding inside the 50-m booth

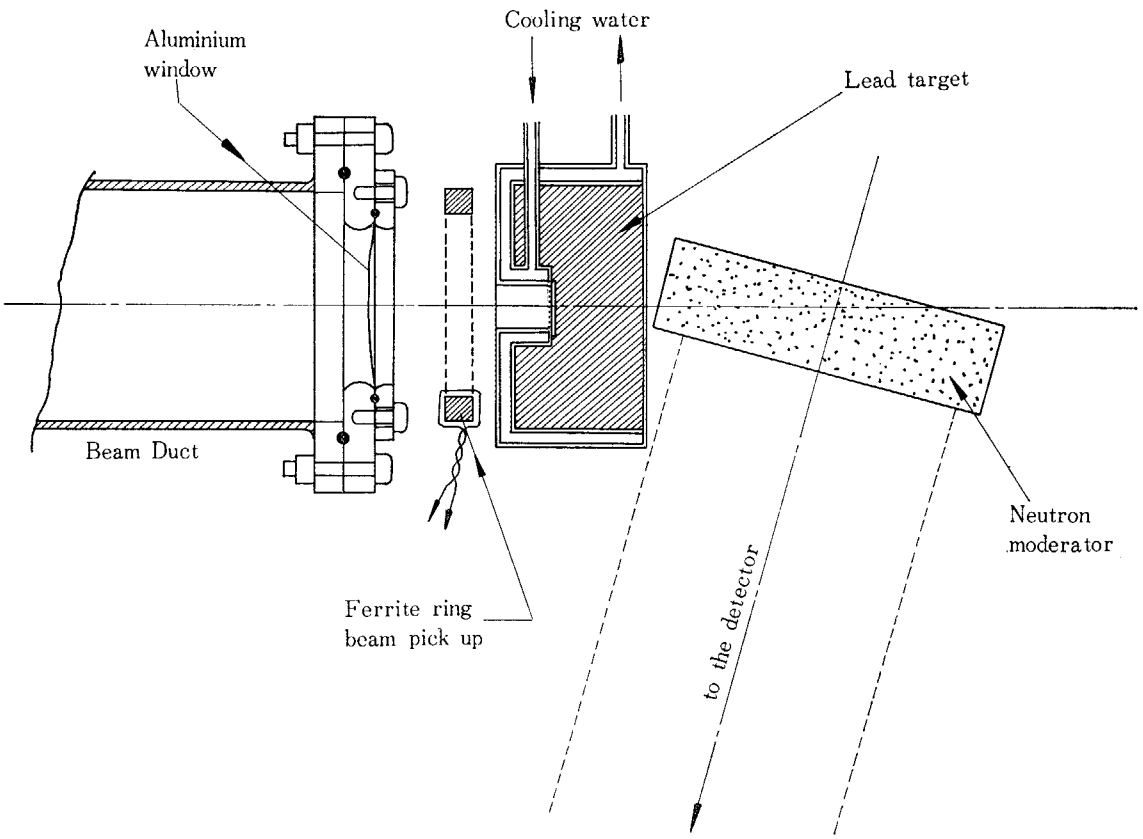

Fig. 3 Schematic figure of the assembly of the photo-neutron source target. In this arrangement, the assembly is placed in such a way that the detector at the 50-m booth cannot see the lead target but the moderator.

and cooled by water flow. A neutron moderator of paraffin block is placed behind the target. To avoid paralysis of the neutron detector by strong gamma-ray flash from the photoneutron target, the detector at the end of the flight path is so arranged as not to view the target but the moderator block. A block of pure paraffin or of mixture of paraffin and boric acid is used as the moderator block when the measurement is made for relatively lower or higher energy neutrons, respectively. The reason for this choice is mentioned later in connection with the background.

3. 2 Flight Path

The 10-m flight path is formed of an aluminium pipe of 6-m length, 320-mm inner diameter and 5-mm wall thickness. The both ends of the pipe have aluminium windows of 0.25mm thickness. The 50-m flight path consists of three pipes: One is a similar pipe as the above and the other two are aluminium pipes each of 6-mm wall thickness, 600-mm i.d., and 20-m length. The aluminium window at the end of the 20-m pipe has 2-mm thickness, which is made rather thicker considering the possibility of accidental destruction of the window at vacuum by any chance. Each flight pipe is evacuated by an oil rotary pump and the vacuum is maintained for a long period without further pumping. Several collimators constructed with lead and paraffin-boric-acid mixture are placed inside of the flight pipes as are shown in Fig. 2 (b).

3. 3 Sample changer

A collimator assembly and a sample changer for transmission measurement are placed between the 6-m and 20-m flight pipes (Fig. 2 (e)). Six samples of $20 \times 20\,cm^2$ cross section at maximum can be mounted on the sample changer. The sample changer is operated automatically by a control circuit, which is also connected with a multichannel time analyzer. The address of the memory of the time analyzer can be divided into 2, 4,. . ., or 2^n with n being an integer, and the above control circuit makes one-to-one correspondence between the divided memory locations and the positions of sample holder in the sample changer. When count of signals from neutron monitor detector reaches a preset count, the position of the sample holder is changed and the memory location for accumulation of signals from the main detector is also changed to a corresponding location. Combination of the positions of the samples in the changer, the memory locations, and the order of the measurements is programmed at a panel of the control circuit of the sample changer, and the measurements of different samples including the case of no sample (open beam) are proceeded automatically in cycles. The number of repetition of the cyclic measurements is registered on a mechanical counter, and its total number can be preset by another mechanical counter.

3. 4 Main detector

The main detector at the end of the 50-m flight path consists of four sets of a ^{6}Li-glass scintillator of $4\frac{3}{8}''$ dia. $\times \frac{1}{4}''$ thickness* (NE 905 or NE 908 of Nuclear Enterprise) and a 5″ dia. photomultiplier of EMI-9579B with an emitter follower circuit. The detector assembly is surrounded by B_4C of about 2 cm thickness and boron loaded paraffin. High voltages to photomultipliers are supplied from a high voltage supply through individual voltage dividers to adjust pulse heights from individual photomultipliers. In order to prevent overloading of circuit due to strong gamma-ray flash from the linac, a diode limitter utilizing the inverse characteristic is connected in series to a coupling condenser between the anode of the photomultiplier and the emitter follower, and a diode is also connected in parallel with the anode resistor. The output of the emitter follower is clipped by a 10-m 3C2V delay line, mixed, clipped again by 10-m 3C2V, and then, entered into a pre-amplifier. The output signal of the preamplifier has a shape of about 0.2-V height and 0.2-μsec width, and is sent to the main amplifier at the control room through an 80-m doubly shielded coaxial cable (5C-2W). After being amplified by the main amplifier with gain of about 40, the signal is entered into a time pick-off and a lower- and an upper-level discriminators. If discrimination of only a lower-level of the signals is made, relatively large time jittering is resulted because of the broad width of pulse-height distribution of neutron signals from the glass scintillator. To reduce the time jittering, therefore, time pick-off is made at a

*This thickness of the scintillator was doubled recently.

level as low as possible, and the output of the time pick-off is made coincidence with the output of the lower discriminator. This coincidence signal is made anticoincidence with the signal from the upper discriminator which is to prevent high level signals from the gamma-ray flash and cosmic rays.

3. 5 Monitor of the neutron beam

The monitor counter consists of an 1″ dia. × 1/8″ ^{6}Li-glass scintillator and a 6292 Dumont photomultiplier, and is mounted in a collimator before the sample changer. The monitor counter is placed not to disturb the neutron beam which directly reaches the main detector, but the monitor is placed in such a way that it can see the moderator of the neutron target. Pre-amplifier output of the monitor signal is sent to an amplifier at the control room. Then, the signal goes through a single-channel pulse-height analyzer, and through a time-gate circuit which permits signals of neutrons in a proper flight-time (energy) range to pass, and then, is sent to a preset scaler whose preset count sets a period of the cyclic measurement of the transmission. The initial delay and the width of the time gate are variable from 0 to 200 μsec and from 0 to 2 msec, respectively. The counting rates of signals of both main detector and the monitor detector are recorded on two electronic pen-recorders. Main circuit units of the above system are all transisterized taking a long term stabilization into consideration.

3. 6 Time analyzer

Acquisition of signals of neutrons from the main detector is made by a 4096-channel TMC analyzer. A block diagram of the analyzer system is shown in Fig. 4. In the figure, number in the parentheses indicates model number of TMC excepting the case where a name of manufacturer is indicated. Description of the section for the pulse-height analysis in the analyzer is omitted in the following. The 4096-channel time-of-flight unit accepts up to four independent inputs. The channels of the TOF unit and the channel width are variable from 16 to 4096 channels in 9 steps and from 0.125 μsec to 64 μsec in 10 steps, respectively. An initial delay variable from 16 to $2^{15} - 16 = 32752$ in unit of the channel width is built-in with the TOF unit. Deadtime of the analyzer for TOF measurement is 2 μsec with a four-word buffer memory, and is 16 μsec without the buffer. There is an auxiliary

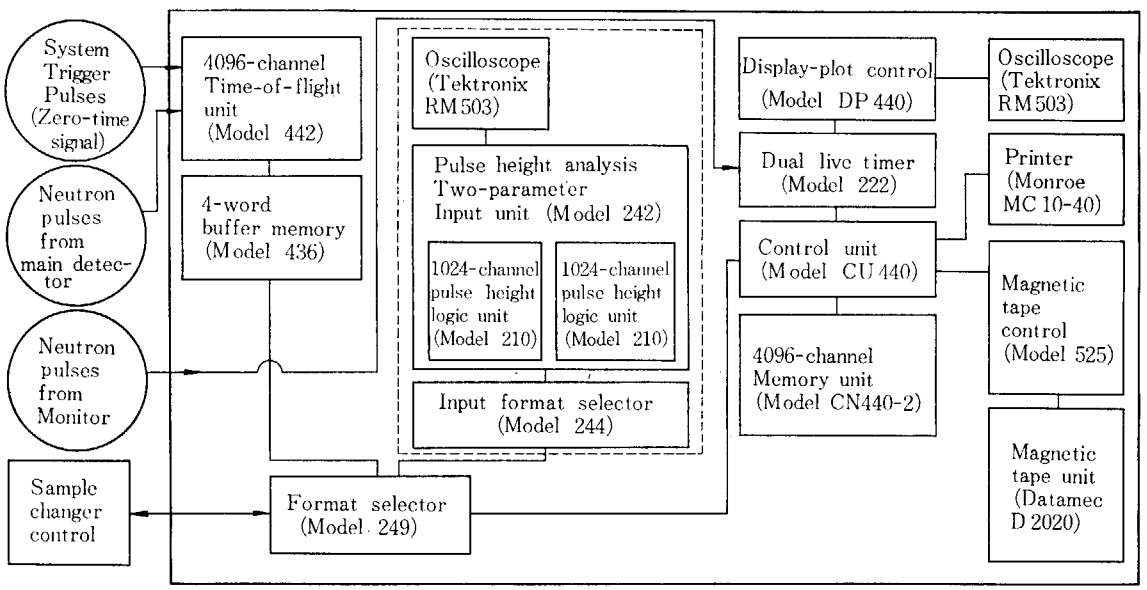

Fig. 4 Block diagram of the 4096-channel analyzer.
Model numbers in the parentheses are given for the convenience of reference.

1024-channel TOF unit which is of one-shot type and whose channel width is variable from 31.25 to 125 nsec. The address of TOF unit is made correspondence with the address of the memory unit at a pin board of the format selector where each terminal corresponds to a bit of the addresses. Each channel of the 4096-channel memory has a capacity of $10^5 - 1$ counts. The time between arrival of a zero-time signal from the ferrite ring and that of a neutron signal from the main detector is measured by the TOF unit. To obtain actual TOF of a neutron, time delay by amplifiers, cables, and other circuit components, which amounts to about one μsec in total, is corrected. Controlling two most significant bits in the 12 bits of the memory address by sample-position indicating signal from the control unit of the sample changer, the 4096 channels are, for example, divided into 4 portions in which the main detector signals for sample-A, sample-B, open-beam, and background measurements are assigned to be accumulated. Read-out of the accumulated data in the analyzer is made by taking a picture of display on oscilloscope with a polaroid camera, by printing the counts with the channel numbers by a fast printer of printing speed of 1040 lines (channels) per minute, and/or by recording them on a magnetic tape. A run number of four figures (four digits), which is set at the control panel of the analyzer, is tagged to the printed data on a paper tape and to the recorded data on a magnetic tape. The final and complete read-out of the data is always made by the magnetic tape unit. A magnetic tape of 1/2-inch width with a standard $10\frac{1}{2}$-inch diameter reel is used. The recording is made with 7 tracks, density of 200 bits per inch, tape speed of 45 inches per second, and with track widths and track-to-track spacings conforming to IBM tape format specifications, and it is an even-parity BCD-coded non-return-to-zero recording. In the magnetic tape recording, a 4096-channel datum is divided into 16 groups of 256 channels each, and a group number (2 characters) and a run number (4 characters) are tagged at the start of each group recording. Six characters are provided for the recording of count in each channel.

4. Characteristics of the spectrometer

4. 1 Pulse-height distribution and efficiency of the detector

In Fig. 5, an example of pulse-height distribution of signals from the ^{6}Li-glass neutron detector is shown. The distribution was taken with a ^{241}Am-Be neutron source embedded in paraffin. A five-cm thick lead block was put in between the neutron source and the glass detector to shield from gamma-rays of the source. FWHM of the pulse-height distribution for neutrons is estimated to be about 40% from the figure.

The cross section of ^{6}Li(n, α)T reaction is known to have 1/v-dependence approximately below neutron energy of 100 keV. Content of ^{6}Li in the glass was evaluated from a measurement of the neutron transmission of the glass. In determining the detector efficiency, the above pulse height distribution of the detector was taken into account. The efficiency of a NE-905 glass detector $4\frac{3}{8}''$ dia. $\times \frac{1}{4}''$ was derived from an experimental transmission of this glass, and is approximately given by $1-\exp(-1.5/\sqrt{E})$ for neutron energy E as shown in Fig. 6. An absolute measurement of spectrum of neutrons from the target can be made by using the above estimated absolute efficiency of the detector.

4. 2 Neutron spectrum and counting rate

The counting rate $C(t)$ and energy spectrum $N(E)$ of the neutron open-beam can be expressed in the following forms:

$$C(t)dt \propto t^{-k}dt, \qquad \text{and} \qquad N(E)dE \propto E^{\frac{k}{2}-1}dE,$$

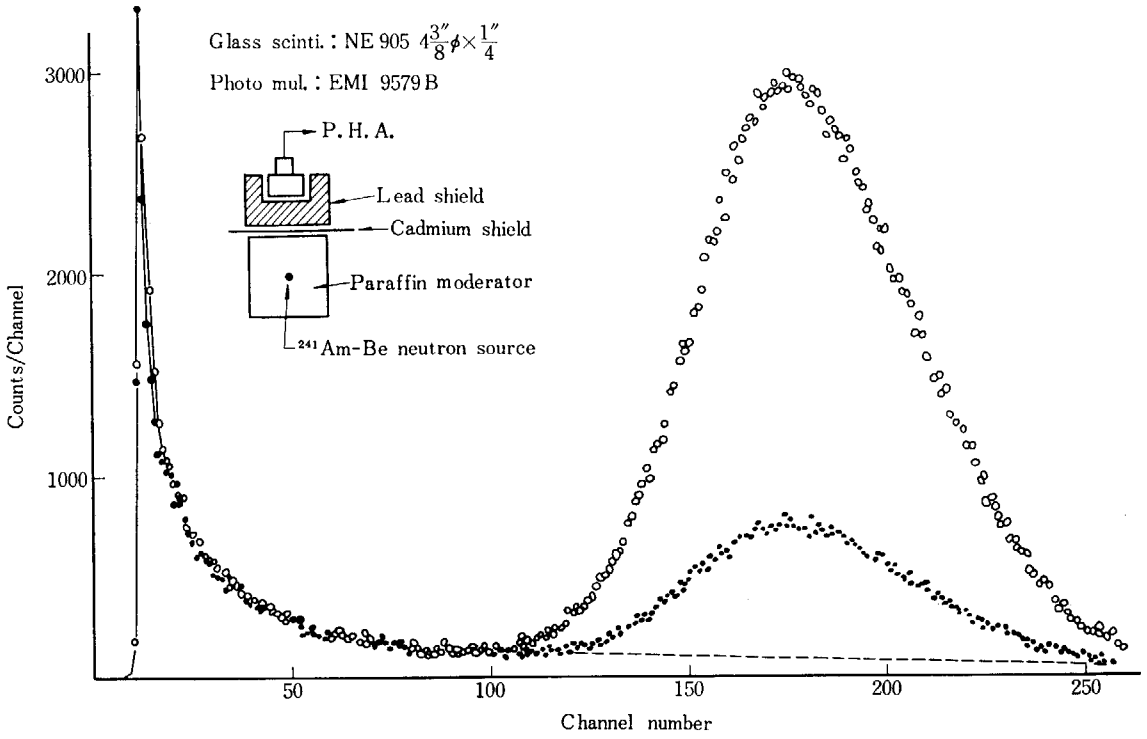

Fig. 5 Pulse-height distribution of signals from a ^{6}Li-glass neutron detector.
The arrangement of the measurement to take this distribution is shown schematically in the figure. The plots with closed and open circles correspond to the measurements with and without cadmium shield between the neutron source and the detector, respectively. From the figure, FWHM of the pulse-height distribution for neutrons is estimated to be about 40%.

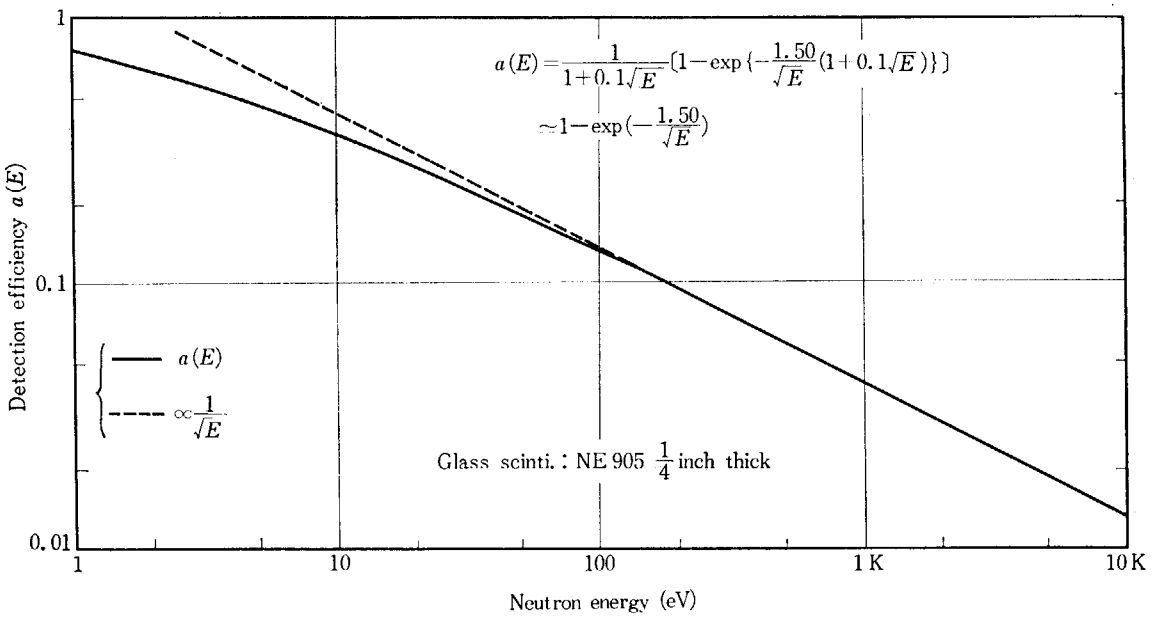

Fig. 6 Neutron detection efficiency of a ^{6}Li-glass scintillator.
Equation for efficiency $a(E)$, which is written in the figure, was derived from the experimental neutron transmission of the glass scintillator.

respectively, where, k is a parameter and was empirically found to be 0.48 ± 0.02 for 10 eV $\lesssim E \lesssim$ 10 keV with the target moderator of moderate thickness. Integrations of the above formula by energy gave results of about 2 neutrons of up to 100 keV and about 3.5 neutrons of up to 1 MeV per cm^2 at 50 m per 4-μsec electron burst with about 80 mA of peak current; and integrations of them for 4π solid angle gave results of 6×10^8 neutrons of up to 100 keV and 1.1×10^9 neutrons of up to 1 MeV per the 4-μsec electron burst. These values are approximately consistent with a value estimated from activation of a gold foil at the target with paraffin moderator enough to thermalize almost all neutrons produced at the target. Some examples of the counting rate are listed in TABLE 1.

TABLE 1 Example of the counting rates of neutrons

Neutron energy (eV)		10	100		1K		10K	
Moderator of the neutron target		Paraffin	Boron loaded paraffin		Boron loaded paraffin		Boron loaded paraffin	
Filter of the beam		Cd 1mm	B_4C(~0.7g/cm^2)		B_4C		B_4C	
Repetition rate of the electron beam pulses		150pps	200pps		200pps		200pps	
Pulse width of the electron beam	(μsec)	4	1	0.5	1	0.5	1	0.5
Channel width of the analyzer	(μsec)	2	1	0.5	1	0.5	1	0.5
	(eV)	0.035	0.55	0.28	18	9	550	280
Counts per channel per minute at 50m		90	17	4	28	6.5	60	14
Background		<1%	≲1%		~1%			~3%

The electron beam current of the linac in these measurements was roughly 80 mA at the peak of the beam pulses.

A sheet of cadmium of 1 mm thickness or a boral plate is usually put into the beam to prevent the overlapping of slower neutrons with neutrons in the next pulse and to increase the repetition rate of the linac pulses. The cadmium filter has a good characteristic of sharp cut-off for slow neutrons but it leaves fine structure of its resonances in the open beam spectrum. The boron filter leaves a smooth open-beam but its thickness sufficient to prevent the overlapping results in fairly large attenuation of good neutrons in lower energy region. The total thickness of the aluminium windows in the beam, which gives rise to resonance dips at 6 keV and 35 keV in the open-beam spectrum, is about 10 mm. In the measured neutron spectrum, there appears a peak at 2.85 keV which was found to be due to the resonance scattering of ^{23}Na in the glass of the photomultiplier of the detector.

4. 3 Background

The strong burst of gamma-rays (gamma-flash) from the linac photo-neutron target excites the glass scintillator, and leaves afterglow in the glass for several hundred microseconds. This causes a strong factor of the background. When the scintillator is exposed directly to the photo-neutron target, random noises comparable in pulse height to the neutron signals remain even several hundred microseconds after arrival of the gamma-flash. The time while the noises of the afterglow have size comparable to or greater than the pulse height for neutron signal is reduced to 50 μsec or 10 μsec when a lead block of 5 cm thickness is inserted in the beam at the above condition or when

the detector sees only the paraffin moderator of the neutron target, respectively. The latter arrangement is adopted in the usual measurements.

The background is measured by inserting a lamination of materials containing elements such as tungsten, cobalt, and manganese into the neutron beam. Each elements in the lamination has the thickness sufficient to black-out the neutron beam at prominent resonances of the elements. The counts at channel regions, where the resonance dips are clearly saturated, are considered to represent the background counts at those respective energies. When the linac is operated with electron-beam width of 4 μsec and the peak current of 100 mA, the background for neutrons below about one keV is almost independent of the time-of-flight and is about twice the natural background. The above linac condition is also applied to the latter explanation about the background. The above-mentioned background for lower-energy neutrons is not reduced by blocking the neutron beam. The main component of background neutrons of energy higher than one keV is presumably resulted from the scattering of neutrons at the inside of the flight tube (collimation system) and at the detector itself and inside of the detector shield. The beam is blocked by a concrete wall behind the detector, but no appreciable effect to the background by scattered neutrons from this wall has been detected. When paraffin block is used as the moderator of the target and when the beam is blocked by a neutron absorber of boron-paraffin mixture, a background component of exponential time dependence is observed. This component is considered to be due to gamma-rays from neutron captures by hydrogen, and the exponential decay corresponds to the life of neutrons in the target moderator. Therefore, this background component is greatly reduced by using the target moderator of boron-paraffin mixture. For measurement of neutron energy below 100 eV, it is better to use paraffin moderator from the viewpoint of the counting rate. In this case, the background is less than one per cent of the open beam.

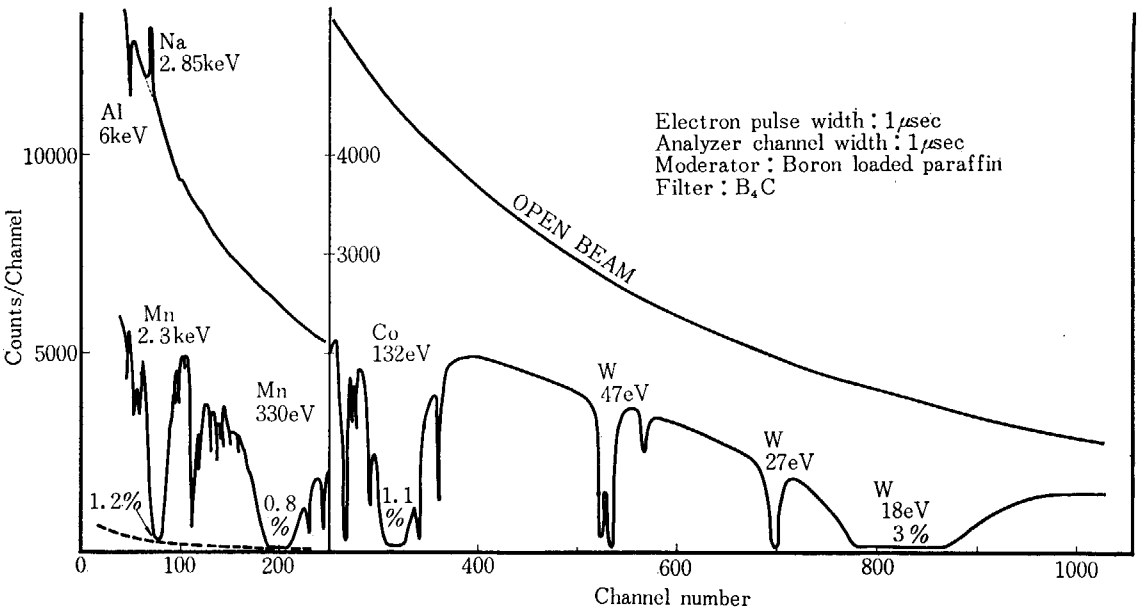

Fig. 7 Transmission spectrum of the black resonance sample and the open-beam spectrum. The lower structural curve indicates the neutron transmission spectrum of the black resonance sample. In the measurement in which these spectra were taken, the pulse width of the linac and the channel width of the analyzer were both 1 μsec and B_4C of about 0.7 gr/cm^2 was inserted in the neutron beam as a filter. The background, which is defined at a black resonance energy as a ratio of counts between conditions when the black resonance sample is in and out for the same count of the beam monitor, is written in the figure at the bottom of each black resonance dip.

For measurement of neutrons above 100 eV, it is effective to use boron-loaded paraffin moderator; and in this case, the background relative to the open beam is 1% at 132 eV (a resonance energy of Co), 0.8% at 330 eV (Mn), 1.2% at 2.3 keV (Mn), and 3% at 35 keV (Al). For higher-energy neutrons, a component of the background under the sample-in condition reduces with increase of the sample thickness. In Fig. 7, TOF spectrum which was taken when the black resonance sample was in the beam is shown in comparison with the open beam spectrum.

4. 4 Energy resolution

The observed neutron transmission $T_{obs}(t)$ for neutrons of TOF t can be written with an instru-

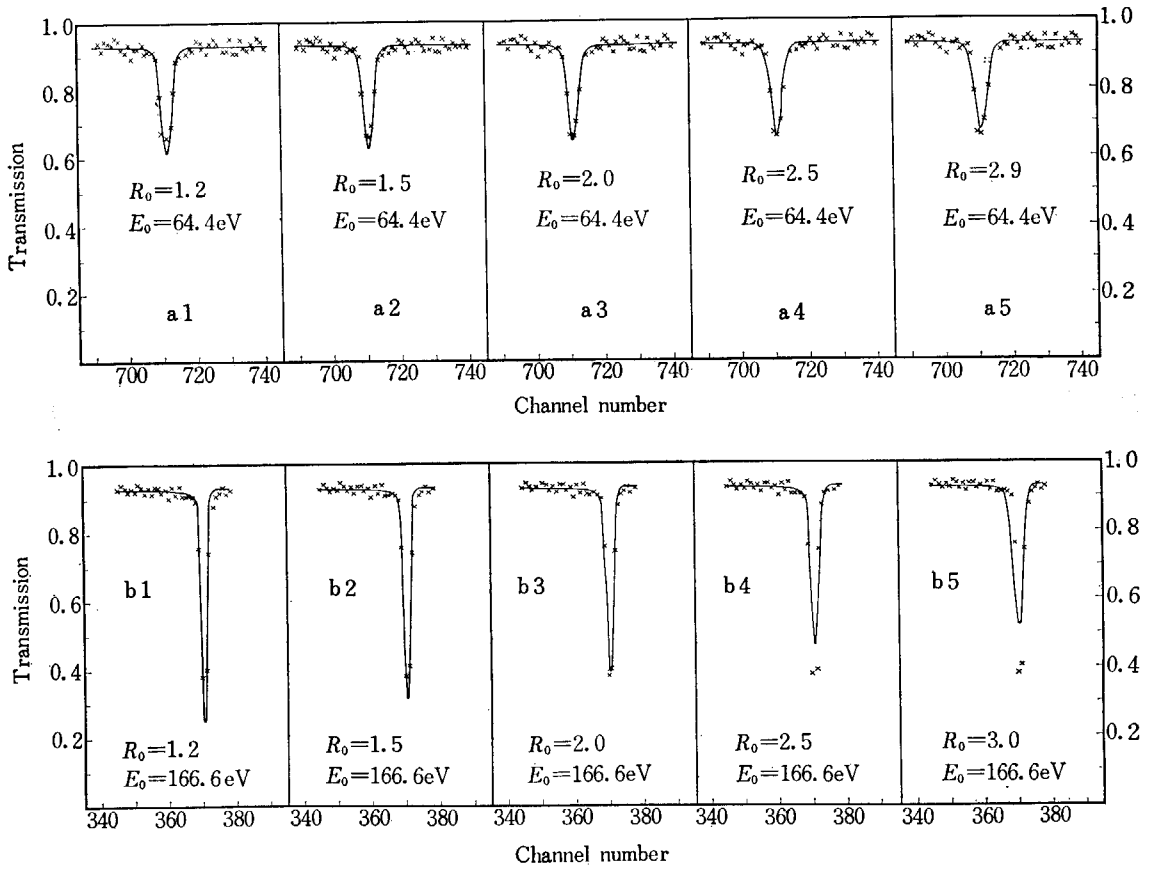

Fig. 8 Comparison of fit of theoretical curves to the experimental transmissions in order to estimate the resolution width.

The experimental transmissions around the resonances at 64.4 eV and 166.6 eV in antimony are plotted by cross points in (a) and (b), respectively. In (a) the same experimental transmissions are plotted through (a1) to (a5) as similar as in (b). The curves represent theoretical transmissions calculated by a computer on the basis of the Breit-Wigner single-level formula and the Gaussian shape of Doppler broadening and resolution function with fixed input parameters of $E_0 = 64.4$ eV, $\Gamma = 90$ mV, and $fg\,\Gamma_n^0 = 0.25\times10^{-4}$ eV for (a) and $E_0 = 166.6$ eV, $\Gamma = 78$ mV, and $fg\,\Gamma_n^0 = 0.35\times10^{-3}$ eV for (b), where E_0, Γ, f, g, and Γ_n^0 are respectively the resonance energy, total width, isotopic content, statistical weight factor, and reduced neutron width.

In the computer calculation, only the resolution width R_0 among the input parameters was changed from (a1) to (a5) and from (b1) to (b5), and the used value of the resolution width in unit of the channel width of the time analyzer is written under the each curve. In the figures, the theoretical curves seem to fit better to the experimental points with $R_0 = 2.0 \pm 0.5$ channels at 64 eV and 1.8 ± 0.2 channels at 167 eV.

mental resolution function $f(t,t')$ and the true (including Doppler broadening) transmission $T(t)$ as follows:

$$T_{ob}(t) = \int_{-\infty}^{\infty} f(t, t')\, T(t')\, dt',$$

where

$$\int_{-\infty}^{\infty} f(t, t')\, dt' = 1.$$

Although it is generally difficult to determine precise shape of $f(t,t')$, adoption of Gaussian function as an approximation of $f(t,t')$ is practically of use for many cases of analyzing the transmission data. In order to check the magnitude of resolution width, experimental transmission curves of resonances were compared with theoretical transmission curves which were computed by using proper resonance parameters* and assumed resolution functions of Gaussian shape with various values of FWHM $= R_0$. In Fig. 8 (a) and (b) are illustrated the comparison of cases for resonances in antimony at 64.4 eV and 166.6 eV, respectively. The theoretical curves were computed by using a computer code[13] which is a modified one from the code written by S. E. ATTA and J. A. HARVEY[14].

The comparison shows that the values of R_0 in unit of the channel width of the time analyzer may be estimated to be 2.0 ± 0.5 channels at 64 eV and 1.8 ± 0.2 channels at 167 eV. The value of the experimental transmission at the depression peak of resonance is sensitive to the accuracy of the background subtraction, and the statistical error of the experimental value at the peak is relatively large. By these reasons, the comparison of the experimental and theoretical curves at the peak of resonance, though the peak value is sensitive to the value of R_0, was not intended.

R_0 depends upon the pulse width $\Delta\tau_e$ of the linac electron beam, channel with $\Delta\tau_c$ of the time analyzer, spread $\Delta\tau_m$ of the moderation time of neutrons in the target moderator, and spread ΔL of the neutron flight-path length L. Using these terms, R_0 at TOF t may be written in the following formula:

$$R_0 = \sqrt{(\Delta\tau_e)^2 + (\Delta\tau_c)^2 + (\Delta\tau_m)^2 + t^2(\Delta L/L)^2}/\Delta\tau_c,$$

in unit of the channel width. Calculated values of R_0 from the above formula with the experimental condition under which the data of Fig. 8 were taken are 2.3 channels at 64 eV and 1.8 channels at 167 eV. In this calculation, $\Delta\tau_m$ is omitted since it is much smaller than the other factors. These values agree reasonably with the ranges of R_0-value estimated from the Fig. 8.

5. Performance

5. 1 Transmission measurement

The observed transmission $T_{ob}(i)$ is defined by the following formula:

$$T_{ob}(i) = \frac{Z_T(i)/M_T - B_T(i)/M_{BT}}{Z_O(i)/M_O - B_O(i)/M_{BO}} = e^{-n\sigma(i)},$$

where, i = a channel number of the TOF at the time analyzer,

$Z(i)$ = the detector count at the channel i during the time in which monitor count reaches M,

$B(i)$ = the background count at the channel i during the time in which the monitor count reaches M_B,

n = the sample thickness, say, in atoms per barn, and

*For an isolated resonance, the resonance parameters with reasonable accuracy can be determined by the area analysis of the experimental transmission without having good knowledge of the resolution.

$\sigma(i)$ = the effective total cross section at the channel i; the effective means that the Doppler broadening and resolution broadening are included.

The suffixes I and O indicate that those symbols Z, B, M, and M_B are measured under the condition of "sample-in" and "sample-out (open-beam)", respectively.

In order to make an accurate measurement of $T_{ob}(i)$ it is important, besides the counting statistics, that the monitor counts M_I, M_{BI}, M_O, and M_{BO} have a precise proportionality with their respective integrated intensities of the neutron beam. To test this proportionality, time variation of the open beam counts per time-analyzer channels per fixed values of the monitor count was examined with changing the linac beam intensity. An example of the result is shown in Fig. 9. In the full energy range of the figure, the proportionality is almost maintained within the statistical accuracy of the examination. When the detector sees directly the photo-neutron target instead of the moderator only, the proportionality is deteriorated at higher neutron energy because of the strong gamma-flash; change of the electron-beam intensity at this condition affects the pulse-height discrimination of the detector pulses and results in the deterioration of the proportionality.

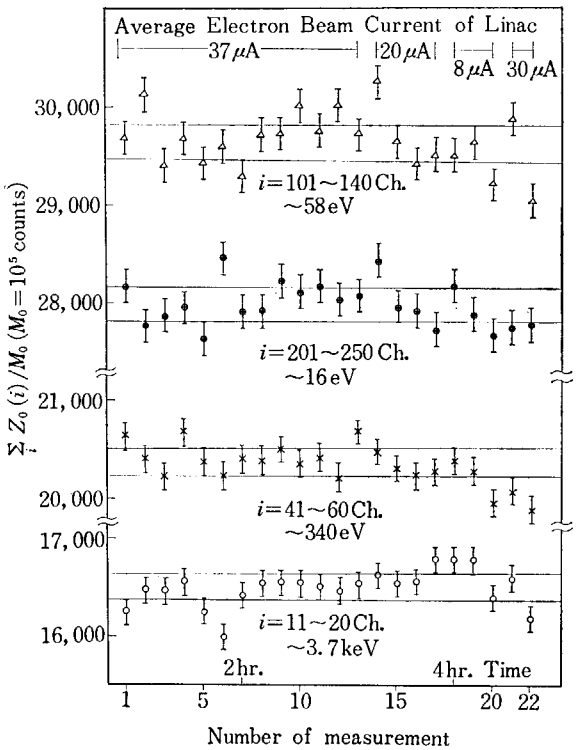

Fig. 9 An example of the proportionality between integrated counts of the main detector and monitor detector.
The ordinate indicates sum of the counts of the main detector in a channel region, which is written in the figure at each set of experimental points, per the same integral count (10^5 counts) of the monitor.
The abscissa indicates the number of measurements.
Time of the measurement is also marked at the inside rim of the abscissa, but the scale is not linear in time. The electron beam energy, width of the beam pulse, the repetition rate, the analyzer-channel width and the flight-path length were 20 MeV, 4 μsec, 125 pps, 4 μsec, and 50 meters, respectively. The neutron energy corresponding to the centre of each channel region is also written in the figure. The electron beam intensity of the linac was changed through the measurements, and the average beam current is shown in the figure at the upper end.

5.2 Processing and analysis of the experimental data[15]

The magnetic tape in which the raw experimental data are recorded by the analyzer is proces-

sed at the Computer Center of JAERI which has IBM 1401 and 7044 computers and is located at about 400 meters from the Linac experimental site. In Fig. 10, the scheme of processing is shown. The

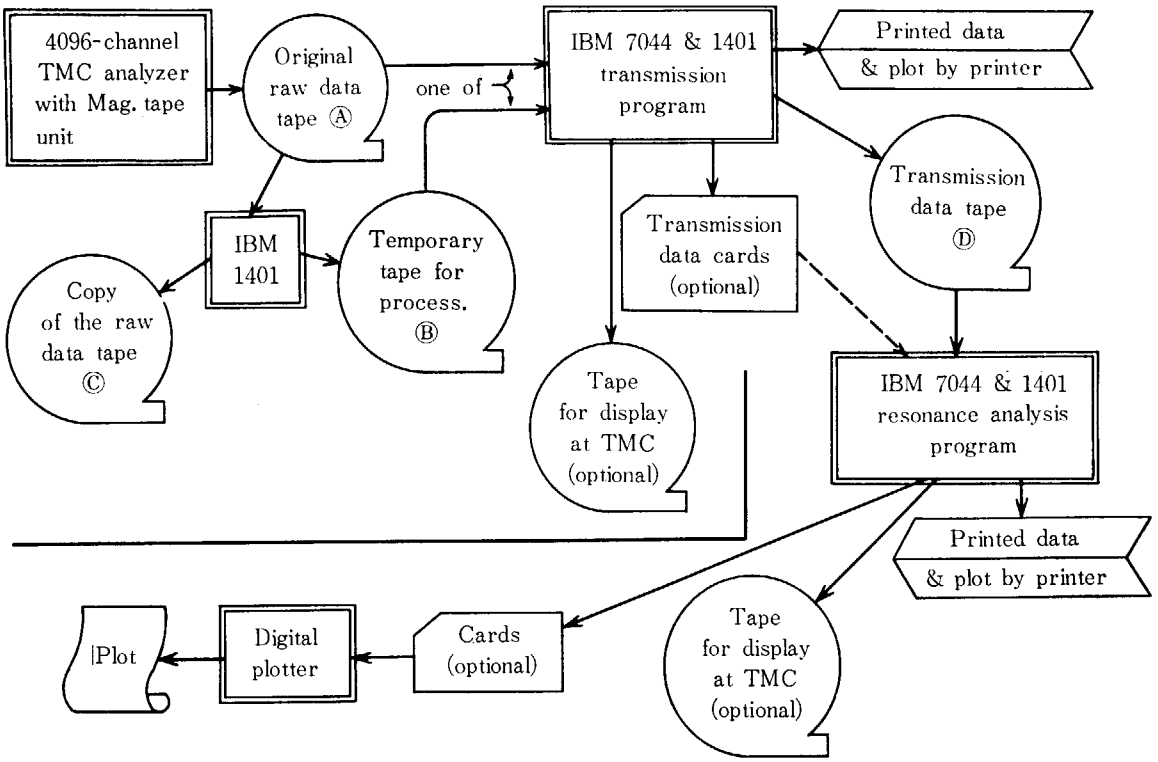

Fig. 10 Schematic flow diagram of processing of the neutron-transmission data from the JAERI Linac TOF Spectrometer.

raw-data tape may be directly fed to the computer as an input-data tape, or the data in the raw-data tape may be selectively transferred to another tape which is to be fed to computer. The raw data are first processed through a programme[16], and the channel-by-channel energy, neutron transmission, its error, total cross section, its error, and so on are computed. In the computation, a correction for deadtime of the analyzer and an inter-calibration among the sets of monitor counts can be included. The expressions of the background for the whole energy range, $B_I(i)$ and $B_0(i)$ are determined by fitting either of the following expressions to the above-mentioned background counts at the black resonances by use of the least-squares method:

$$B(i) = b_o + \frac{b_1}{i} + \frac{b_2}{l^2} + \cdots\cdots,$$

or

$$B(i) = b_0 + b_1 e^{-b_2 i} + b_3 e^{-b_4 i},$$

where b_0, b_1, $\cdots$ are parameters and suffixes I and 0 are omitted for the sake of simplicity. The output magnetic tape from the computation with the above programme contains the channel-by-channel transmissions and their errors, and this tape is fed to the computer as an input tape for further analysis on neutron resonances. For this, a programme[13], which is a modification from the area-analysis programme written by ATTA and HARVEY[14], and the shape-analysis programme by ATTA and HARVEY[14] are used. In the modified area-analysis programme, computation of neutron-width value is made regeneratively until a sum of assumed gamma-width and computed neutron-width converges to total-width value which is estimated from the previous result in an automatic repetition, and experimental errors of transmissions at individual channels are taken into account in the calculation of an error of the computed neutron-width value.

At the present stage of our experiments, the read-out of the multichannel-analyzer data by a magnetic tape with a format compatible to a computer input furnishes a step efficient enough in our data-processing scheme. In a transmission experiment, main part of the total time consumption consists in the analysis of a number of resonance dips to obtain the resonance parameters, and this is resulted not from the net computer time for the analysis but rather from the waiting time for the computer runs, since many computer runs are required rather than the computer-time of each run, and from the man time in preparation for the computer inputs which may include parameters determined from result of the preceding computation. Therefore, a considerable weight should still be put on a continuous effort to develope the data processing including computer programme.

5. 3 Transmission data

Examples of the transmission data are shown in Fig. 11. The measurements were made on metallic antimony samples of several different thicknesses up to 55 mm. The data in Fig. 11 (a) and (b) were taken with resolution of about 20 and 10 nsec/m, respectively. It is one of the reasons to make the transmission measurements with various sample thicknesses that total-widths beside neutron-width, hence gamma-widths, can also be determined by the thick-thin method in favourable cases.

Acknowledgements

The authors wish to thank Dr. T. MOMOTA for his advice, encouragement, and support. They are indebted to Mr. T. KURITA for his contribution in designing the flight path, and to the operating staff of the Linac Laboratory for valuable assistance in the operation of the Linac.

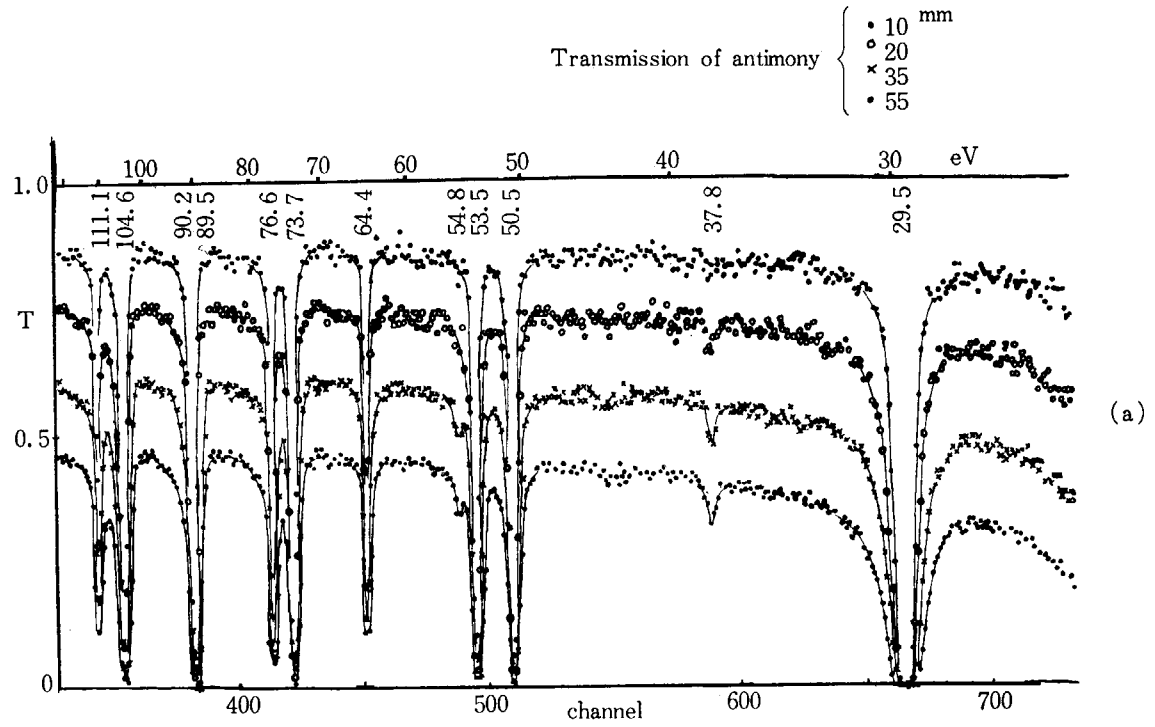

Fig. 11 The neutron transmission data of natural antimony.
The data of (a) and (b) were taken with resolution of about 20 and 10 nsec/m, respectively. Thicknesses of the samples and neutron energy are indicated in the figure.

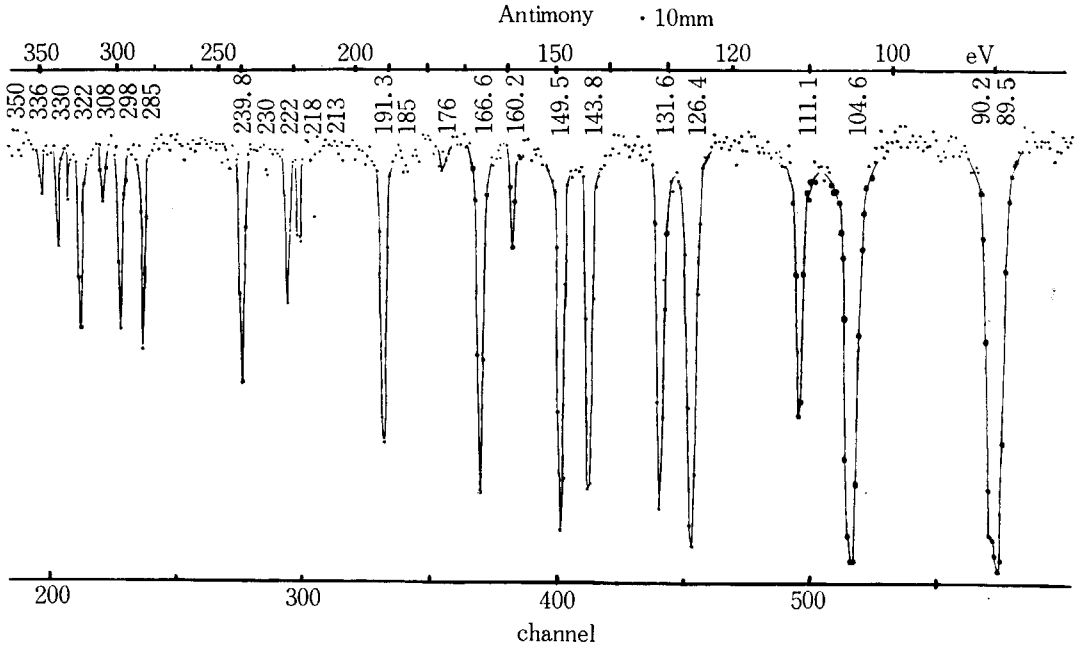

(b)

References

1) E. P. WIGNER: *ORNL-2309*, 59 (1956) unpublished; *Canadian Mathematical Congress Proceedings*, 174 (1957) unpublished; and *Columbia Uuiv. Report CU-175*, 49 (1957) unpublished.
2) C. E. PORTER and R. G. THOMAS: *Phys. Rev.*, 104, 483 (1956).
3) J. D. GARRISON: *Ann. Phys.* (N. Y.), 30, 269 (1964).
4) K. K. SETH: *Nuclear Phys.*, 47, 169 (1961); J. JULIEN, S. DE BARROS, V. D. HUYNH, G. POITTEVIN, J. MORGENSTERN, F. NETTER et C. SAMOUR: *Nuclear Phys.*, 66, 433 (1965); and J. JURIEN, S. DE BARROS, G. BIANCHI, C. CORGE, V. D. HUYNH, G. LE POITTEVIN, J. MORGENSTERN, F. NETTER, C. SAMOUR et R. VASTEL: *Nuclear Phys.*, 76, 391 (1966).
5) R. E. CHRIEN, H. H. BOLOTIN and H. PALEVSKY: *Phys. Rev.*, 127, 1680 (1962); L. M. BOLLINGER, R. E. COTE, R. T. CARPENTER and J. P. MARION: *Phys. Rev.*, 132, 1640 (1963); R. E. SEGEL, R. K. SMITHER, and R. T. CARPENTER: *Phys. Rev.*, 133, B583 (1964); H. E. JACKSON: *Phys. Rev.*, 134, B931 (1964); and H. E. JACKSON, J. JULIEN, C. SAMOUR, A. BLOCH, C. LOPATA and J. MORGENSTERN: *Phys. Rev. Letters*, 17, 656 (1966).
6) A. SAPLAKOGLU, L. M. BOLLINGER and R. E. COTE: *Phys. Rev.*, 109, 1258 (1958); P. RIBON et A. MICHAUDON: *J. Phys. radium*, 24, 987 (1963); H. E. JACKSON: *Phys. Rev.*, 131, 2153 (1963); L. M. BOLLINGER and G. E. THOMAS: *Phys. Letters*, 8, 45 (1964); and K. G. MCONEILL, D. B. MCCONNELL and F. W. K. FIRK: *Can. J. Phys.*, 43, 2156 (1965).
7) A. M. LANE and J. E. LYNN: *Nuclear Phys.*, 17, 563 and 586 (1960); and O. A. WASSON and J. E. DRAPER: *Phys. Letters*, 6, 350 (1963) and *Nuclear Phys.*, 73, 499 (1965).
8) C. SHAKIN: *Ann. Phys.* (N. Y.), 22, 373 (1963); B. BLOCK and H. FESHBACH: *Ann. Phys.* (N. Y.), 23, 47 (1963); T. FUKETA, F. A. KHAN and J. A. HARVEY: *ORNL-3425*, 36 (1963); H. IKEGAMI and G. T. EMERY: *Phys. Rev. Letters*, 13, 26 (1964); J. A. FARRELL, G. C. KYKER, JR, E. G. BILPUCH and M. W. NEWSON: *Phys. Letters*, 17, 286 (1965); and H. FESHBACH, A. K. KERMAN and R. H. LEMMER: *Ann. Phys.* (N. Y.), 41, 230 (1967).
9) J. RAINWATER, W. W. HAVENS, JR., and J. B. GARG: *Rev. Sci. Instr.*, 35, 263 (1964).
10) F. W. K. FIRK, G. W. REID and J. F. GALLAGHER: *Nuclear Instr.*, 3, 309 (1958); F. W. K. FIRK: *Nuclear Instr. and Methods*, 28, 205 (1964); M. ASGHAR, C. M. CHAFFEY, M. C. MOXON, N. J. PATTENDEN, E. R. RAE and C. A. UTTLEY: *Nuclear Phys.*, 76, 196 (1966); and M. ASGHAR, C. M. CHAFFEY and M. C. MOXON: *Nuclear Phys.*, 85, 305 (1966).
11) J. A. HARVEY: *Private communication;* and *ORNL*-3924, 145 (1966).
12) Linear Accelerator Laboratory, JAERI: *JAERI*-6014 (1964) in Japanese.
13) A. TACHIBANA, T. IWAKI, A. ASAMI, E. KIMURA, Y. NAKAJIMA and T. FUKETA: to be published in *JAERI Memo.*
14) S. E. ATTA and J. A. HARVEY: *ORNL*-3205 (1961) and its Addendum (1963).
15) T. FUKETA, A. ASAMI, M. OKUBO, Y. NAKAJIMA, Y. KAWARASAKI and H. TAKEKOSHI: *CN*-23/17, Conf on Nuclear Data, Paris, Oct. (1966).
16) E. KIMURA, A. ASAMI, Y. NAKAJIMA and T. FUKETA: to be published in *JAERI Memo.*